XVIII. PROCESSING AND TRANSMISSION OF INFORMATION*

Prof. W. B. Davenport, Jr.	Dr. A. Wojnar	A. R. Hassan
Prof. P. Elias	T. Adcock	J. L. Holsinger
Prof. R. M. Fano	T. M. Anderson	T. S. Huang
Prof. R. G. Gallager	M. H. Bender	R. S. Kennedy
Prof. F. C. Hennie III	E. F. Berlekamp	L. Kleinrock
Prof. E. M. Hofstetter	J. E. Cunningham	A. H. Molin
Prof. D. A. Huffman	H. Dym	J. E. Savage
Prof. I. M. Jacobs	P. M. Ebert	J. R. Sklar
Prof. A. M. Manders	D. Ecklein	I. G. Stiglitz
Prof. B. Reiffen	D. D. Falconer	I. E. Sutherland
Prof. W. F. Schreiber	E. F. Ferretti	W. R. Sutherland
Prof. C. E. Shannon	G. D. Forney, Jr.	O. J. Tretiak
Prof. J. M. Wozencraft	U. F. Gronemann	W. J. Wilson
Dr. C. L. Liu	P. W. Hartman	H. L. Yudkin

RESEARCH OBJECTIVES

This group continues its investigation of sources that generate information, channels that transmit it, and machines that process it.

Work is continuing on the processing of pictures by means of computers. The broad objective of this work is to elucidate the fundamental properties of vision as they apply to image transmission and reproduction. Among the more specific objectives are the design of efficient image-transmission systems, and the development of devices capable of performing some "human" operations, such as noise reduction, image detection, and quality improvement.

The efficient transmission of speech by digital means is also receiving some attention. The objective of this work is the early exploitation for speech communication of digital transmission systems employing encoding and decoding.

During the past year, significant new results have been obtained on the properties of sequential encoding and decoding, and on feedback strategies for noisy two-way channels. Increased emphasis is being placed on the exploitation of these techniques in conjunction with physical channels, and on the design of the necessary encoding and decoding equipment. Plans for the future include the development of acoustic channels capable of simulating multipath and scattering phenomena of practical interest, and of encoding and decoding equipment sufficiently flexible to permit experimentation in real time in conjunction with these channels.

An effort is being made to bring into sharper focus the relation between the newer encoding techniques and older modulation schemes. For this purpose, the behavior near threshold of frequency modulation and pulse-position modulation are being investigated by experimental, as well as analytical, means.

Work continues, also, on the structural characteristics of digital machines. A prime objective of this work is the establishment of relations among the reaction time of machine, the complexity of the data processing to be performed, the number of storage elements, and the speed of the elementary components.

R. M. Fano, D. A. Huffman, W. F. Schreiber, J. M. Wozencraft

*This research was supported in part by Purchase Order DDL B-00368 with Lincoln Laboratory, a center for research operated by Massachusetts Institute of Technology, with the joint support of the U.S. Army, Navy, and Air Force under Air Force Contract AF19(604)-7400; and in part by the National Institutes of Health (Grant MH-04737-02).

(XVIII. PROCESSING AND TRANSMISSION OF INFORMATION)

A. PICTURE PROCESSING

1. A STUDY OF THE PICTURE-SAMPLING PROCESS

Every picture-transmitting system involves a stage in which an electric signal is abstracted from a source image, and a stage in which the electric signal is converted to another image. The first of the above-mentioned stages may be thought of as a sampling process, and the second as a filtering operation.

If the picture-transmitting system is one that sends a sequence of signal values (sampled data), the over-all system may be modeled as the block diagram shown in Fig. XVIII-1. While this block diagram is not a good description of all possible image-transmission systems, many systems do fit our model. Note that the input function is a function of two dimensions (space) if the picture is a photograph, and of two spatial dimensions and time for a real image. The present study is restricted to still pictures; thus the filters and functions are defined on two variables – they are two dimensional.

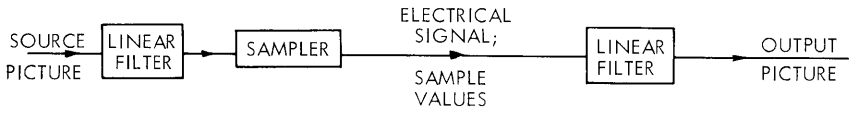

Fig. XVIII-1. Diagram of image-transmission system.

The purpose of this study is to investigate the effect of the impulse responses of the two linear filters in Fig. XVIII-1 on the quality of the transmitted picture. The experiments will be performed with the digital television equipment built by our group.[1] The filter used before sampling is synthesized by defocusing the scanner lens, and placing a transparency on the lens. The impulse response of such an optical system is just the transmittance distribution of the transparency on the lens. The linear filter that converts the sample values into the final picture is a similar combination of defocused lens and transparency in the recording camera.

O. J. Tretiak

References

1. J. W. Pan, U. F. Gronemann, T. S. Huang, J. E. Cunningham, and W. F. Schreiber, Picture Processing Research, Quarterly Progress Report No. 61, Research Laboratory of Electronics, M. I. T., April 15, 1961, p. 133.

2. THE MATHEMATICAL FOUNDATION OF THE SYNTHETIC HIGHS SYSTEM

The Synthetic Highs[1] system is a channel-capacity reduction technique that is useful for efficient coding of television signals. Figure XVIII-2 illustrates the logic used, and Figure XVIII-3 shows waveforms illustrating the underlying principle. Figure XVIII-3a

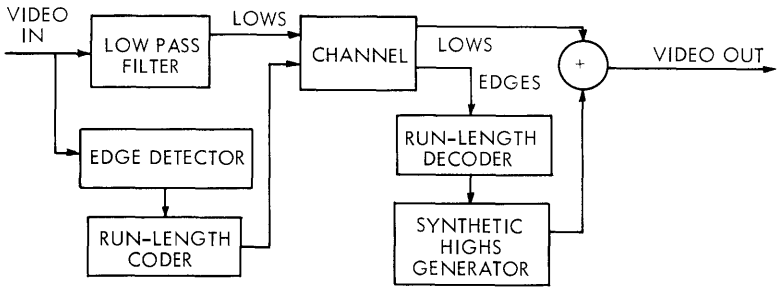

Fig. XVIII-2. Diagram of Synthetic Highs system.

is an exemplary video signal. The low-frequency component (Fig. XVIII-3b) is transmitted conventionally. The edge detector is essentially a differentiator, giving the output, (Fig. XVIII-3c). This signal is transmitted by some form of run-length coding, put back in real time by the decoder, and applied to the synthetic highs generator (a linear filter) to produce the waveform (Fig. XVIII-3d). This waveform is added to the transmitted lows to produce the output video.

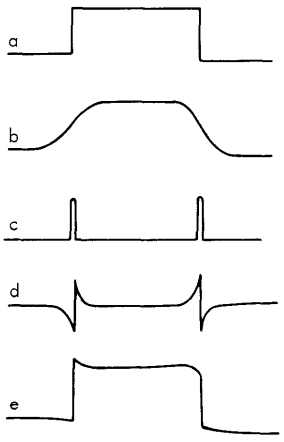

Fig. XVIII-3. Waveforms of Synthetic Highs system.

It has always been evident from qualitative considerations that if the edge detection (differentiation), coding, and decoding were error-free, then a linear filter could be found to generate a high-frequency component to produce a video output identical with the input.[2] This has been confirmed by experiment, but never proved mathematically. The purpose of this note is to present a proof and to extend the theory to two- and three-dimensional coding.

a. One-dimensional Case

Consider a picture whose brightness as a function of position is called B(x). If the spatial impulse response of the lowpass filter is M(x), and the output of the edge

detector is dB/dx, then we have the problem of finding a filter whose impulse response H(x) satisfies the following equation:

$$\int \frac{dB(x')}{dx} H(x-x')\, dx' = B(x) - \int B(x')\, M(x'-x)\, dx'. \tag{1}$$

Put into words, the edge signal dB/dx is applied to the filter H, and the output is to be the high-frequency component of the original video, expressed as the entire signal minus the low-frequency component. This equation is solved by taking transforms of both sides. sides. Thus

$$j\omega\, b(\omega)\, h(\omega) = b(\omega) - b(\omega)\, m(\omega). \tag{2}$$

As long as $b(\omega) \neq 0$,

$$j\omega\, h(\omega) = 1 - m(\omega). \tag{3}$$

Taking inverse transforms, we obtain

$$\frac{dH}{dx} = u_o(x) - M(x) \tag{4}$$

$$H(x) = u_{-1}(x) - \int_{-\infty}^{x} M(x')\, dx' \tag{5}$$

which is precisely the result that was obtained experimentally.

b. Two-Dimensional Case

Since the correlation between vertically disposed picture elements is fully as great as that between horizontally disposed elements, it is clear that increased savings are available by extending the technique to two dimensions. The first successful attempt to do this was reported by a member of our group recently.[3] In his work, John W. Pan detected both horizontal and vertical edges and transmitted them to the receiver by fitting a series of straight lines to the outlines of objects in the picture. The high-frequency signal was synthesized in terms of either a vertical or horizontal edge, whichever was closer to the fitted line segment. Artifacts occurred at the corners of objects and along contours of approximately 45°, the former being partially eliminated by a special "rounding" routine.

An alternative procedure suggests itself in connection with the preceding mathematical derivation. Suppose that we use a system very similar to that in Fig. XVIII-2, but in which the filters are two-dimensional, the edge detector is a contour detector, and the run-length coder is some form of contour tracer and coder. The question then arises about whether there is a two-dimensional filter into which one can put data on the contours of an image (such data being efficiently codable) and out of which one might obtain the two-dimensional high-frequency component of the image. The filter should

be invariant with the image so that all possible images might be handled without introducing spurious artifacts in special cases such as at corners of objects. It has been found possible to solve this problem if the gradient of the image, ∇B is used as an edge detector, and if the filter is specified by its vector impulse response.

The output of the filter, which is the scalar high-frequency component, is then defined as the dot product convolution of the input ∇B and the response H. Thus we have a relation analogous to (1) to define H.

$$\nabla B \odot \overline{H} = B - B \otimes M, \tag{6}$$

where $\otimes$ is the conventional scalar convolution, and $\odot$ is the dot product convolution. Taking the transform of both sides, we have

$$[j\overline{\omega}\, b(\overline{\omega})] \cdot \overline{h}(\omega) = b(\overline{\omega}) - b(\overline{\omega})\, m(\overline{\omega}). \tag{7}$$

For $b \neq 0$,

$$j\overline{\omega} \cdot \overline{h} = 1 - m(\overline{\omega}) \tag{8}$$

which, by rule (A-5) in the Appendix, can now be retransformed into the space domain to yield

$$\nabla \cdot \overline{H} = u_o(\overline{r}) - M(\overline{r}). \tag{9}$$

We solve for $\overline{H}$ by integrating throughout the circle of radius r.

$$\int_0^{2\pi}\int_0^r \nabla \cdot \overline{H}\, r\, dr d\theta = \int_0^{2\pi}\int_0^r [u_o(\overline{r}) - M(\overline{r})]\, r\, dr d\theta = 1 - \int_0^{2\pi}\int_0^r M(\overline{r})\, r\, dr d\theta \tag{10}$$

We simplify this equation by assuming radial symmetry and by applying the divergence theorem to the left-hand side.

$$\oint_r \overline{H} \cdot \hat{n}\, r\, d\theta = 1 - 2\pi \int_0^r L(\overline{r})\, rdr$$

$$\overline{H} \cdot \hat{r}\, 2\pi r = 1 - 2\pi \int_0^r L(\overline{r})\, rdr \tag{11}$$

$$\overline{H} = \hat{r}\left[\frac{1}{2\pi r} - \frac{1}{r}\int_0^r L(\overline{r})\, rdr\right] \tag{12}$$

This general result indicates that it is possible to implement the system of Fig. XVIII-2 in two dimensions. The reconstructed picture should be identical to the original if the gradient field is transmitted without error. Previous experience with the tolerance of human vision to errors caused by nonexact gradient transmission in one dimension indicate that quite high efficiency; that is, more than ten-to-one reduction in data rate

should be possible with quite small quality impairment. To achieve this, it will be necessary to fit curves of at least second degree to the detected gradient points, so that discontinuous second derivatives of the outlines may be avoided.

c. Three-Dimensional Case

The relation (9) is valid for any number of dimensions, since it was derived in vector form, the only restriction being the transformability of the function involved. We may thus solve for $\overline{\overline{H}}$ in three dimensions, assuming radial symmetry,

$$\int_r \nabla \cdot \overline{\overline{H}}\, dV = 1 - \int_r L(\bar{r})\, dV, \tag{13}$$

where $\int_r dV$ signifies a volume integral within the sphere of radius r. Again using the divergence theorem, we obtain

$$\int_r \overline{\overline{H}} \cdot \hat{n}\, dS = 1 - \int_r M(\bar{r})\, dV \tag{14}$$

$$\overline{\overline{H}} \cdot \hat{f}\, 4\pi r^2 = 1 - \int_r M(\bar{r})\, dV \tag{15}$$

$$\overline{\overline{H}} = \frac{\hat{r}}{4\pi r^2}\left[1 - \int_r M(\bar{r})\, dV\right]. \tag{16}$$

The three-dimensional situation arises when we deal with images that change in time. The input is then B(x, y, t). From our analysis, it appears possible to reconstruct B(x, y, t) at the receiver by combining a low-frequency component (that is, a low-definition, low frame-rate picture) with a synthetic highs component. The last component is found from the dot product convolution of the transmitted gradient and a spatio-temporal filter $\overline{\overline{H}}$.

To economize on the transmission of the gradient data, presumable it would be possible to perform a contour-tracing operation and then transmit a few parameters of the contours. In this case, the "contours" would be surfaces rather than curves.

It is evident that the restriction to radially symmetrical three-dimensional filters means that the errors introduced into the space and time domains of the moving image which are due to quantizing errors, will be similar. Since the spatial and temporal frequency responses of human vision, as deduced from threshold measurements, are similar in shape (some worker believe they are physiologically related) it is to be expected that similar distortions will be similarly acceptable.

APPENDIX

FOURIER TRANSFORMS IN VECTOR NOTATION

1. Introduction

Using capitals to represent functions in the space domain and lower case letters for their corresponding transforms, we have

$$\bar{r} = x\hat{i} + y\hat{j}$$

$$\bar{\omega} = \omega_x\hat{i} + \omega_y\hat{j}$$

$$\bar{H}(r) = \bar{H}(x, y) = H_x\hat{i} + H_y\hat{j}.$$

(Do not confuse $j = \sqrt{-1}$ with $\hat{j}$, the unit vector in the y or ω_y direction.)

We define the two-dimensional transform

$$\bar{m}(\omega) = \iint M(\bar{r})\, e^{-j\bar{\omega}\cdot\bar{r}}\, dA.$$

Here, dA is the area element in the space domain. On this basis, and using the linearity properties of Fourier transforms, we have

$$\bar{h}(\bar{\omega}) = h_x(\bar{\omega})\hat{i} + h_y(\bar{\omega})\hat{j}$$

$$= \hat{i}\iint H_x(\bar{r})\, e^{-j\bar{\omega}\cdot\bar{r}}\, dA + \hat{j}\iint H_y(\bar{r})\, e^{-j\bar{\omega}\cdot\bar{r}}\, dA$$

$$\bar{h}(\bar{\omega}) = \iint \bar{H}(\bar{r})\, e^{-j\bar{\omega}\cdot\bar{r}}\, dA$$

which we write

$$\bar{h}(\bar{\omega}) \Longleftrightarrow \bar{H}(\bar{r}) \tag{A-1}$$

$$h_x(\bar{\omega}) \Longleftrightarrow H_x(\bar{r}) \tag{A-2}$$

$$h_y(\bar{\omega}) \Longleftrightarrow H_y(\bar{r}). \tag{A-3}$$

2. Differential Operators

Since $h(\bar{\omega}) = \iint H(\bar{r})\, e^{-j\bar{\omega}\cdot\bar{r}}\, dA$, it can be shown for reasonable H's that

$$H(\bar{r}) = \iint h(\bar{\omega})\, e^{j\bar{\omega}\cdot\bar{r}}\, \frac{d\Omega}{(2\pi)^2},$$

where $d\Omega$ is the area element in the frequency domain. Thus

$$\frac{\partial H}{\partial x} = \iint j\omega_x h(\bar{\omega})\, e^{j\bar{\omega}\cdot\bar{r}}\, \frac{d\Omega}{(2\pi)^2}$$

$$\frac{\partial H}{\partial y} = \iint j\omega_y h(\bar{\omega})\, e^{j\bar{\omega}\cdot\bar{r}}\, \frac{d\Omega}{(2\pi)^2}.$$

Since $\nabla H = \hat{i}\frac{\partial H}{\partial x} + \hat{j}\frac{\partial H}{\partial y}$, we have

$$\nabla H = \iint j\bar{\omega} h(\bar{\omega})\, e^{j\bar{\omega}\cdot\bar{r}}\, \frac{d\Omega}{(2\pi)^2}$$

$$\boxed{\nabla H \Longleftrightarrow j\bar{\omega} h} \qquad \text{(A-4)}$$

If $\bar{H}$ is a vector, so that $H_x \Longleftrightarrow h_x$, then $\frac{\partial H_x}{\partial x} \Longleftrightarrow j\omega_x h_x$, and so on.

Since $\nabla \cdot \bar{H} = \frac{\partial H_x}{\partial x} + \frac{\partial H_y}{\partial y} = \iint j(\omega_x h_x + \omega_y h_y)\, e^{j\bar{\omega}\cdot\bar{r}}\, \frac{d\Omega}{(2\pi)^2}$

$$\boxed{\nabla \cdot \bar{H} \Longleftrightarrow j\bar{\omega}\cdot\bar{h}} \qquad \text{(A-5)}$$

3. Convolutions

In multidimensional space, we can take convolutions among vectors, scalars or vectors and scalars. It is of interest to find the equivalent operation in the frequency domain to these various convolutions in the space domain. By strict analogy with the one-dimensional use, we have

$$P \otimes Q \Longleftrightarrow pq \qquad \text{(A-6)}$$

$$\bar{P} \otimes Q \Longleftrightarrow \bar{p}\bar{q}, \text{ where } \otimes \equiv \text{scalar convolution.} \qquad \text{(A-7)}$$

Since $\bar{P}\cdot\bar{Q} = P_x Q_x + P_y Q_y$,

$$\bar{P} \odot \bar{Q} \Longleftrightarrow \bar{p}\cdot\bar{q}, \qquad \text{(A-8)}$$

where $\odot \equiv$ scalar product convolution.

W. F. Schrieber

References

1. W. F. Schreiber, C. F. Knapp, and N. D. Kay, Synthetic Highs – an experimental TV bandwidth reduction system, SMPTE J. 68, 525 (1959)

2. In practice, the motivation for using this technique is that for statistical and psychophysical reasons, it is possible to make substantial economies in the transmission of the edge signal without serious image degradation. These economies involve, among other things, the introduction of quantizing errors into the edge transmission.

3. J. W. Pan, Picture processing, Quarterly Progress Report No. 66, Research Laboratory of Electronics, M. I. T., July 15, 1962, p. 229.

B. FREQUENCY-COMPRESSIVE FEEDBACK SYSTEMS

1. Introduction

The main purpose of this research project is to extend the analysis of a signal-tracking FM system[1] which has recently been applied successfully in space communication. A system with a frequency-compressive feedback loop around the frequency demodulator was devised[2] as early as 1939, but its applications did not appear until the late 1950's, and, in fact, a careful analysis was not begun until the appearance of Enloe's paper,[3] in 1962. Enloe's prediction of the second threshold in the closed loop seems to be qualitatively correct; the purpose of the present research is to provide a quantitative verification.

In order to extend the analysis of threshold phenomena in FM systems, an attempt has been made to develop new formulas for determining the input and output signal-to-noise ratios at the "threshold of full improvement." Thus, we seek to bridge the gap between exact analysis (leading to complex nondiscussible expressions) and elementary approximations with limited validity.

Our final aim is to prescribe the synthesis procedure for optimum FM reception filters and to determine the power-bandwidth "trade-off" relations.

2. Threshold in the Conventional System

Threshold in an FM system is the transition region between linear and nonlinear input-output behavior, as well as between Gaussian and non-Gaussian output noise domains. Early progress in analyzing the FM threshold phenomena has been achieved mainly by the very complex computations of Rice[4,5] and Stumpers.[6] Rice's results were exploited by Skinner,[3] who produced the threshold curves of the conventional FM system with ideal filters and an ideal demodulator.

Skinner's plot[3] clearly shows that the carrier-to-noise power ratio (CNR) producing the threshold (of full improvement[7]) depends on filter bandwidths and can hardly be considered constant. The widely assumed existence of a fixed threshold CNR leads inevitably to errors of approximately 5 db, or more.

To facilitate the analysis of the real, sliding threshold, we propose a new simple expression:

$$r_t' = \frac{B_{IF}}{B_{LF}} ,$$

where r_t' is the demodulator input CNR at the threshold (in the if band), B_{IF} is the equivalent two-sided noise bandwidth of the predemodulator filter, and B_{LF} is the equivalent noise bandwidth of the postdemodulator filter.

Comparison of this formula with the Skinner-Replogle[8] exact threshold curves shows

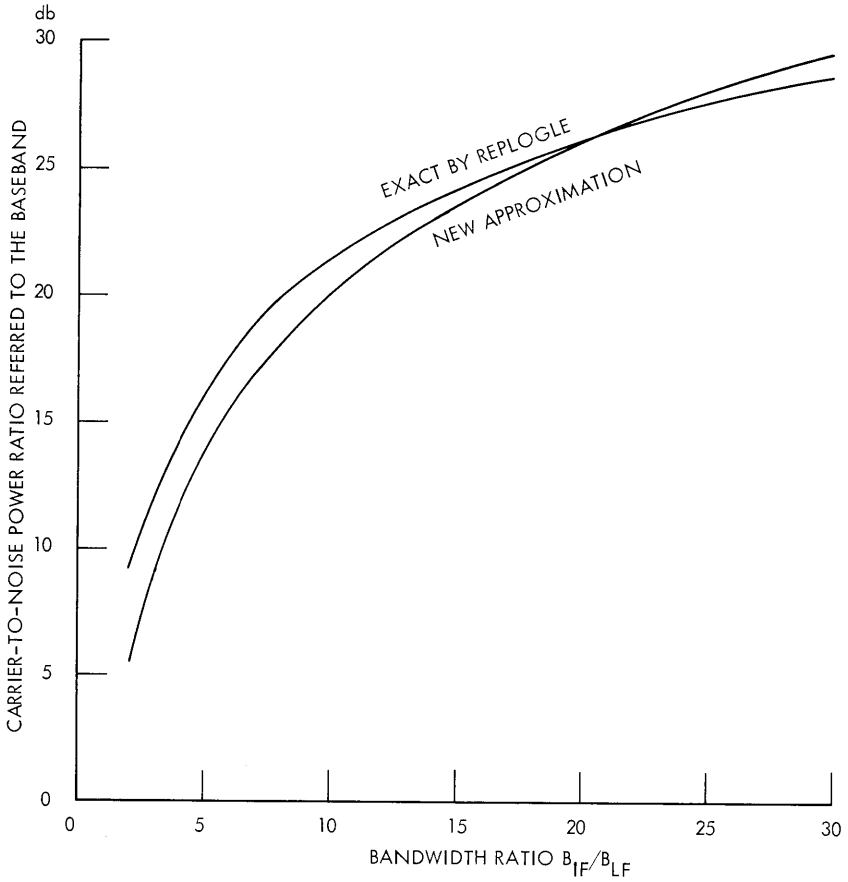

Fig. XVIII-4. Comparison of the new expression for threshold carrier-to-noise power ratio in the baseband with the Skinner-Replogle exact threshold curve.

that now the errors do not exceed 2 db in the very wide range

$$\frac{B_{IF}}{B_{LF}} = 3 \div 30.$$

(See Fig. XVIII-4.)

The well-established expression for output signal-to-noise power ratio at and above the threshold of full improvement is

$$R = \frac{3}{2} m^2 r,$$

where both the input CNR, denoted r, and the output SNR, denoted R, are determined in a bandwidth that is equal to the baseband; m denotes the modulation index of an FM signal. Hence, we obtain a new formula for SNR at threshold:

$$R_t = \frac{3}{2} m^2 r_t = \frac{3}{2} m^2 \left(\frac{B_{IF}}{B_{LF}}\right)^2.$$

Let us also assume that the if filter of nearly rectangular shape has a noise bandwidth equal to the approximate bandwidth of the FM signal:

$$B_{IF} = B_S \cong 2f_m(1+m),$$

where f_m denotes the baseband width or the maximum modulating frequency. Then, with the postdemodulator filter also matched to the baseband ($B_{LF}=f_m$), we obtain

$$r_t \approx 4(1+m)^2$$

$$R_t \approx 6m^2 (1+m)^2.$$

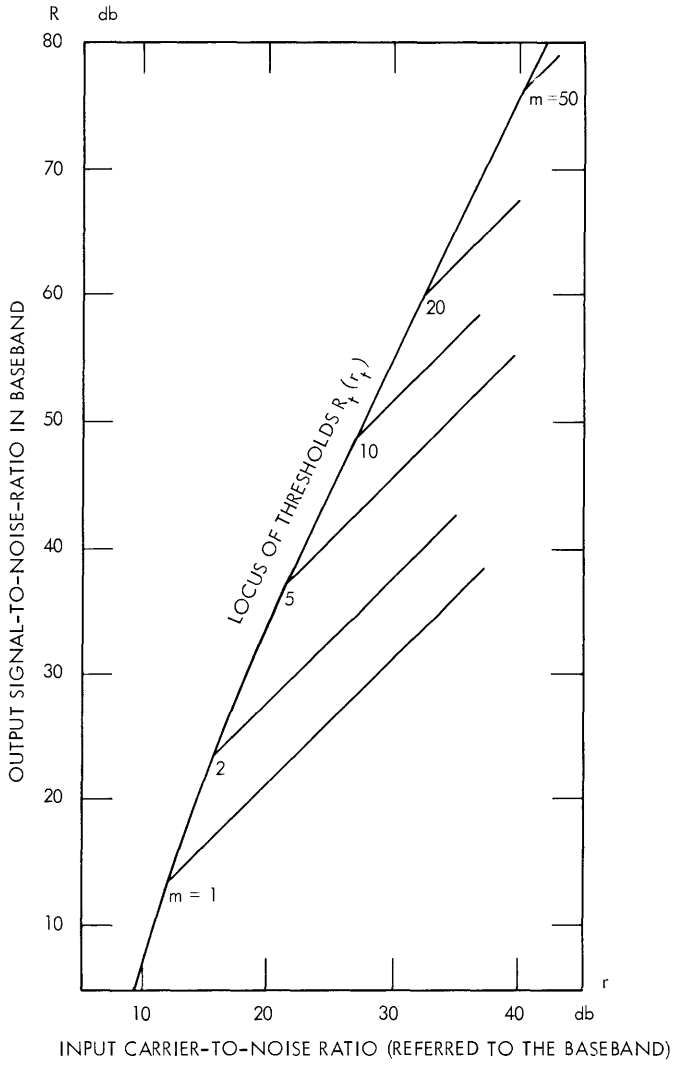

Fig. XVIII-5. Optimum conventional FM systems.

This set of simple but fairly accurate formulas can be used to analyze quantitatively the threshold behavior in a conventional FM system. Note, for instance, that if the signal power, the noise power spectral density, and the baseband remain fixed, there exists a unique minimum value of the signal modulation index

$$m_{min} = \sqrt{\sqrt{\frac{R_t}{6}} + \frac{1}{4} - \frac{1}{2}},$$

which will yield the required system output performance R_t with minimum signal-bandwidth consumption.

Since r_t and R_t are strictly interrelated in an optimal fashion, we can represent all optimal conventional systems by a single locus (Fig. XVIII-5)

$$R_t = \frac{3}{2} r_t \left(\frac{r_t}{4} - \sqrt{r_t} + 1 \right).$$

Each point on the locus graph corresponds to one value of the signal characteristic

$$m = \frac{1}{2} \sqrt{r_t} - 1.$$

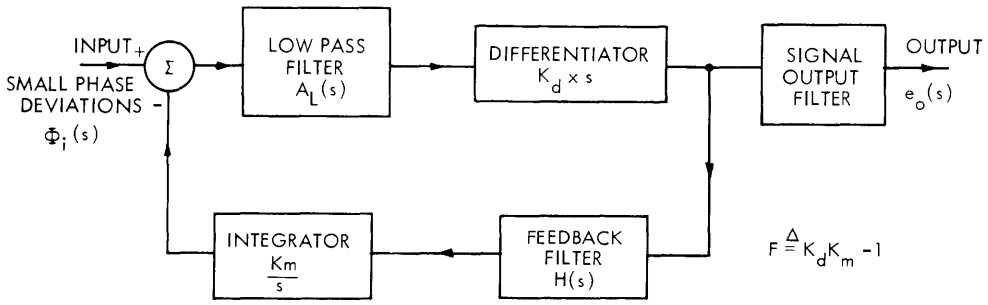

Fig. XVIII-6. Linearized baseband analog for a frequency-compressive FM system.

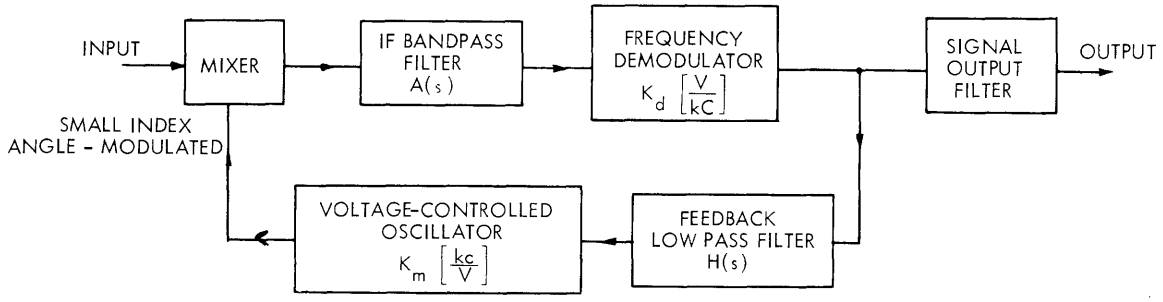

Fig. XVIII-7. Block diagram for a frequency-compressive feedback FM system.

3. Thresholds in the Frequency-Compressive Feedback System

In order to analyze the threshold behavior in the frequency-compressive feedback loop, we adopt Enloe's reasoning and results.[3,8] In particular, the fundamental limitation in exchanging power and bandwidth is believed to occur because of the so-called closed-loop feedback threshold.

When using the linearized baseband analog (Fig. XVIII-6) of the actual system (Fig. XVIII-7) note that a variety of feedback filter structures is possible, but for the if filter the single-pole bandpass structure is imposed by stability requirements. Enloe has found that the input noise in quadrature with the carrier produces angle noise modulation of the variable oscillator. If the rms phase deviation of this noise modulation is no longer small compared with unity, a new (feedback) threshold occurs.

As a measure for the location of this feedback threshold, Enloe suggested the input carrier-to-noise ratio ρ_c in the closed-loop noise bandwidth B_c, and evaluated it as

$$\rho_c = 5\left(\frac{F-1}{F}\right)^2,$$

where F is the feedback factor, which equals the frequency deviation compression ratio. Noise bandwidth B_c must be defined for the transfer from signal input to the oscillator input of the mixer.

The last formula may easily be translated to the customary baseband width f_m, and it becomes

$$\rho = 5\left(\frac{F-1}{F}\right)^2 \times \frac{B_c}{f_m}.$$

This threshold CNR can now be directly compared with the conventional (so-called open-loop) threshold r_t that occurs in the usual way in the frequency demodulator, preceded by a narrow-band if filter. Since both thresholds are independent, it is obvious that maximum system sensitivity occurs with $\rho = r_t$. This condition can be met by proper location of transfer poles around the feedback loop.

When positioning the pole of the if filter the compression of the signal modulation index, which is now m/F in the if path, should be implemented. Thanks to the reduction of nonlinear distortion in the feedback loop, it is no longer necessary that the signal bandwidth equal the filter noise bandwidth.[8] It is now sufficient to make the analog single-pole filter natural frequency, $a/2\pi$, equal to the if signal-frequency deviation, mf_m/F. Hence

$$\frac{a}{2\pi} = f_m \frac{m}{F}$$

and with the if filter noise bandwidth $B_{IF} = \frac{a}{2}$, we find

$$\frac{B_{IF}}{f_m}\Big| = \pi \frac{m}{F},$$

so that for the conventional threshold,

$$r_t = \left(\frac{B_{IF}}{f_m}\right)^2 \approx 10\left(\frac{m}{F}\right)^2.$$

The closed-loop noise bandwidth B_c depends for the most part on the structure and parameters of the feedback filter. With certain simple structures, however, a proportional relation of the type $B_c \approx 2 f_m F$ is approximately valid. In this case we have

$$\rho \approx 10 \frac{(F-1)^2}{F}.$$

To fulfill the condition of maximum sensitivity, $\rho = r_t$, we then require

$$10\left(\frac{m}{F}\right)^2 = 10 \frac{(F-1)^2}{F}.$$

From this equation, we obtain the optimum signal index

$$m_{opt} = (F-1)\sqrt{F}$$

for a most sensitive feedback system with the compression ratio F. If the output performance R_t is prescribed, there is then no choice for F except

$$F_{opt} = 1 + \sqrt[4]{\frac{R_t}{15}} = 1 + 0.51\sqrt[4]{R_t},$$

and algebraically we can find

$$\rho = \frac{5.1\sqrt{R_t}}{1.97 + \sqrt[4]{R_t}}.$$

Now, a power comparison of the threshold r_t of a conventional FM system with that of a feedback system (ρ) is straightforward. Of course, equal performance R_t of both systems at the threshold should be assumed:

$$R_t = \frac{3}{2}m^2 r_t = \frac{3}{2}m_F^2 \rho,$$

where the subscript F pertains to the feedback system. Since for the conventional system, then, we have

$$r_t = \left(1 + \sqrt{1+2\sqrt{\frac{2}{3}R_2}}\right)^2$$

the extension of threshold amounts to

$$\frac{r_t}{\rho} = \frac{\left(1 + \sqrt{1+2\sqrt{\frac{2}{3}R_t}}\right)^2}{5.1R_t \Big/ \left(1.97+\sqrt[4]{R_t}\right)}.$$

Assuming, for example, that $R_t = 10^4$, or 40 db, we obtain the following feedback system parameters.

$$F_{opt} = 1 + 5.1 \sqrt[4]{10^4} = 6.1$$

$$m_{F_{opt}} = 5.1 \sqrt{6.1} = 12.6.$$

The power saving, in comparison with the standard system is, then

$$\frac{r_t}{\rho} = 4.5, \text{ or } 6.5 \text{ db.}$$

Note that there is actually a trade-off between bandwidth and power, since the signal bandwidth increases proportionally as $1 + m_F$. This leads to

$$\frac{B_{S_F}}{B_S} = \frac{1+m_F}{1+m} = \frac{1+(F-1)\sqrt{F}}{\sqrt{\sqrt{\frac{R_t}{6}}+\frac{1}{4}+\frac{1}{2}}}.$$

In our example, it amounts to

$$\frac{B_{S_F}}{B_S} = \frac{13.6}{6.9} = 1.97,$$

that is, the 6.5-db power saving will require a 97 per cent increase in spectrum occupancy. It is, however, not the best trade-off obtainable with an optimally designed feedback filter.

4. Optimization of the Feedback Loop

For the feedback loop to be stable and to have finite noise bandwidth, it is necessary to interrelate the number of poles and the number of zeros in the open-loop transfer function. Two choices are possible: the number of poles exceeds the number of zeros

by 1 (this gives a better stability margin), or the number of poles exceeds the number of zeros by 2 (this is still stable, although with a smaller margin).

Practical tests have shown that three poles in the open loop, excluding the chain of broadband if amplifiers, is the upper limit. It is known, also, that only one pole is allowed in the narrow-band if filter for stability reasons. Therefore one need only consider the following structures for the feedback filter: 1p; 1p and 1z; 2p and 1z; 2p and 2z.

In this list, the class with one zero can be subdivided into two groups: the zero cancels the if filter pole, and the zero does not cancel the if filter pole. The latter will subsequently be called a stabilizing zero. It is obvious that in the "2p and 2z" filter, one zero is of the cancelling type and the other of the stabilizing type.

The main requirements for the optimum feedback loop synthesis are: (a) open-loop transfer function should be reasonably uniform over the baseband (in order to have the if frequency deviation compressed for all modulation frequencies); and (b) closed-loop noise bandwidth should be minimized by a judicious choice of the feedback filter structure and of the location of its stabilizing zero.

It is important to note again that the closed-loop transfer and bandwidth are defined between the two inputs of the mixer (Fig. XVIII-7). The closed-loop transfer function $H_c(s)$ is uniquely determined by the open-loop transfer function $H_o(s)$.

$$H_c(s) = \frac{H_o(s)}{1 + H_o(s)}.$$

The definition of the closed-loop noise bandwidth that has been adopted is

$$B_c = \frac{1/2\pi j}{[H_c(0)]^2} \int_{-j\infty}^{j\infty} H_c(s)\, H_c(-s)\, ds$$

and the integration can easily be performed for rational transfer functions.[9]

In particular, the open-loop transfer function of the highest permitted order has the form

$$H_o(s) = \frac{a}{s+a} \times \frac{b}{s+b} \times \frac{s+c}{c} \times (F-1),$$

which directly corresponds to the most general "2p and 2z" case, and also to the "1p and 1z" (stabilizing) case. Then the closed-loop transfer function is

$$H_c(s) = \frac{ab(F-1)(s+c)/c}{s^2 + [a+b+ab(F-1)/c]\, s + abF},$$

and the closed-loop noise bandwidth can be shown to be

$$B_c = \frac{abF}{2(a+b)} \times \frac{c^2 + abF}{c^2 + abc(F-1)/(a+b)}$$

It is now possible to prove that there is only one choice of value for c to minimize B_c:

$$c_{opt} = \frac{F}{F-1}\left[(a+b)+\sqrt{(a^2+b^2)+ab(F+1/F)}\right].$$

After tedious algebraic manipulations, we obtain the minimum noise bandwidth of the closed-loop with an optimum stabilizing zero

$$B_{c_{min}} = \frac{abF^2}{c_{opt}(F-1)} = \frac{abF}{a+b+\sqrt{a^2+b^2+ab\left(F+\frac{1}{F}\right)}}.$$

This is a quite general result of considerable interest for the system design.

In the apparently best "2p and 2z" class of feedback filters, there are two special cases of particularly advantageous performance. The following simple expressions hold true for the binomial filter with two cascaded real poles, a = b,

$$c_{opt} = b\frac{F+\sqrt{F}}{\sqrt{F}-1}; \qquad B_{c_{min}} = b\frac{F\sqrt{F}}{(1+\sqrt{F})^2}$$

For the Butterworth filter, with two conjugate poles, we denote

$$a = \frac{A}{\sqrt{2}}(1+j) \qquad b = \frac{A}{\sqrt{2}}(1-j) = -aj$$

and it follows that

$$c_{opt} = \frac{AF}{F-1}\left(\sqrt{2}+\sqrt{F+\frac{1}{F}}\right)$$

$$B_{c_{min}} = \frac{AF\sqrt{F}}{\sqrt{F^2+1+\sqrt{2F}}}$$

Other possible filter structures have been catalogued during this work together with their noise bandwidths. The determination of the feedback-filter parameters with regard to the baseband width will be the subject of further study.

In order to prepare an orientation for the expected results, we shall continue with the example given above for the optimum Butterworth filter. If we assume that half-power bandwidth of the open-loop transfer function coincides with the highest modulation frequency f_m, we must set $A = 2\pi f_m$. Consequently,

$$\frac{B_{c_{min}}}{f_m} = \frac{2\pi F}{\sqrt{F + \frac{1}{F} + \sqrt{2}}}$$

and

$$r_{t_F} = \rho = \frac{10\pi(F-1)^2/F}{\sqrt{F + \frac{1}{F} + \sqrt{2}}}.$$

Furthermore, it can be found that

$$R_t = \frac{150(F-1)^4}{\left(\sqrt{F + \frac{1}{F} + \sqrt{2}}\right)^2}.$$

Solving this for F, with $R_t = 10^4$ as before, we obtain

$$F_{opt} = 6.74$$

wherefrom

$$m_{F_{opt}} = 13.2 \quad \text{and} \quad \rho = 38.0.$$

Finally, the power saving is evaluated as 7 db at the expense of a 106 per cent increase in signal bandwidth. Note that the efficiency of power-bandwidth exchange remains virtually unaffected by the optimization of the feedback filter.

5. Direction of Further Study

After the final choice of the best filter structure, the design procedure for the feedback filter will be formulated. Then the optimization problem of the feedback system will be resolved. The analytical results will be summarized in a general chart in which the optimum system parameters m_F, F will be indicated, as well as the system performance at threshold in terms of r_t and R_t. The expected threshold extension will also be obtainable from the chart.

Preliminary measurements have resulted in qualitative agreement with the analysis. The principal analytical conclusions will undergo a comprehensive experimental verification.

The author gratefully acknowledges the aid and encouragement of Professor John M. Wozencraft. Many helpful suggestions from Professor L. A. Gould and Professor E. M. Hofstetter are also appreciated. This part of the research project was performed while the author was working under a Ford Foundation Postdoctoral Fellowship.

A. Wojnar

References

1. C. L. Ruthroff, Project Echo: FM demodulators with negative feedback, Bell System Tech. J. 40, 1149 (1961).

2. J. G. Chaffee, The application of negative feedback to frequency-modulation systems, Bell System Tech. J. 18, 404 (1939).

3. L. H. Enloe, Decreasing the threshold in FM by frequency feedback, Proc. IRE 50, 18 (1962).

4. S. O. Rice, Mathematical Analysis of random noise, Bell System Tech. J. 24, 46 (1945).

5. S. O. Rice, Properties of sine wave plus noise, Bell System Tech. J. 27, 109 (1948).

6. F. L. H. M. Stumpers, Theory of frequency-modulation noise, Proc. IRE 36, 1081 (1948).

7. M. Schwartz, Signal-to-noise effects and threshold effects in FM, Proc. National Electronic Conference, Vol. 18, p. 59, 1962.

8. L. H. Enloe, The synthesis of frequency feedback demodulators, Proc. National Electronic Conference, Vol. 18, p. 477, 1962.

9. G. C. Newton, L. A. Gould, and J. F. Kaiser, Analytical Design of Linear Feedback Controls (John Wiley and Sons, Inc., New York, 1957).